Evidence that lipid lateral phase separation induces functionally significant structural changes in the Ca^{+2}ATPase of the sarcoplasmic reticulum

Francisco J. Asturias,* Donatella Pascolini,‡ and J. Kent Blasie*
*Department of Chemistry, University of Pennsylvania, Philadelphia, Pennsylvania 19104; and ‡The Wistar Institute, Philadelphia, Pennsylvania 19104 USA

ABSTRACT We have studied lipid lateral phase separation (LPS) in the intact sarcoplasmic reticulum (SR) membrane and in bilayers of isolated SR membrane lipids as a function of temperature, $[Mg^{+2}]$, and degree of hydration. Lipid LPS was observed in both the intact membrane and in the bilayers of isolated SR lipids, and the LPS behavior of both systems was found to be qualitatively similar. Namely, lipid LPS occurs only at relatively low temperature and water content, independently of the $[Mg^{+2}]$, and the upper characteristic temperature (t_h) for lipid LPS for both the membrane and bilayers of its isolated lipids coincide to within a few degrees. However, at similar temperatures, isolated lipids show more LPS than the lipids in the intact membrane. Lipid LPS in the intact membrane and in bilayers of the isolated lipids is fully reversible, and more extensive for samples partially dehydrated at temperatures below t_h. Our previous x-ray diffraction studies established the existence of a temperature-induced transition in the profile structure of the sarcoplasmic reticulum Ca^{+2}ATPase which occurs at a temperature corresponding to the $[Mg^{+2}]$-dependent upper characteristic temperature for lipid LPS in the SR membrane. Furthermore, the functionality of the ATPase, and in particular the lifetime of the first phosphorylated enzyme conformation ($E_1 \sim P$) in the Ca^{+2} transport cycle, were also found to be linked to the occurrence of this structural transition. The hysterisis observed in lipid LPS behavior as a function of temperature and water content provides a possible explanation for the more efficient transient trapping of the enzyme in the $E_1 \sim P$ conformation observed in SR membranes partially dehydrated at temperatures below t_h. The observation that LPS behavior for the intact SR membrane and bilayers of isolated SR lipids (no protein present) are qualitatively similar strongly suggests that the LPS behavior of the SR membrane lipids is responsible for the observed structural change in the Ca^{+2}ATPase and the resulting significant increase in $E_1 \sim P$ lifetime for temperatures below t_h.

INTRODUCTION

Previous x-ray diffraction studies of the sarcoplasmic reticulum (SR)[1] membrane from our laboratory revealed the existence of a temperature-induced structural transition in the rotationally averaged profile structure of the Ca^{+2}ATPase protein, and established a correlation between the upper characteristic temperature for lateral phase separation (1) of the membrane lipids, t_h, and the temperature at which the structural transition in the protein was observed (2, 3). The temperature-induced changes observed in the lamellar diffraction and corresponding profile structure of the SR membrane at low $[Mg^{+2}]$ are illustrated, for example, in Fig. 1 (3). These studies related the occurrence of the structural transition in the protein to significant changes in its Ca^{+2}-transport function, as manifested, for example, in a significant extension below the transition temperature of the lifetime of the first phosphorylated enzyme intermediate, $E_1 \sim P$, in the Ca^{+2} transport cycle of the SR. This is illustrated in Fig. 2 (4). Our conclusions concerning the functional relevance of these structural changes observed in the membrane were further supported by our study of the effect of $[Mg^{+2}]$ on the profile structure of the SR membrane, the value of t_h, and the kinetics of Ca^{+2} uptake by the SR system (3).

By studying the effects of several different physico-chemical parameters on the lateral phase separation (LPS) behavior of the lipids in the intact SR membrane, we expected to be able to firmly establish the existence of a relation between the behavior of the lipids and the structure and functionality of the Ca^{+2}ATPase, the latter measured by the kinetics of ATP-induced Ca^{+2} uptake. We had previously studied the kinetics of Ca^{+2} uptake by both multilayers (relatively low water content) and vesicular dispersions (relatively high water content) of SR membranes (3, 4), and found some differences that we attributed to changes in the degree of hydration of the membranes. Our previous studies on the influence of different physico-chemical parameters on the LPS behavior of the lipids in the intact SR membrane (3) did not

[1] *Abbreviations used in this paper:* $E_1 \sim P$, first phosphorylated enzyme intermediate in the Ca^{+2} transport cycle of the Ca^{+2}ATPase protein; *I*, diffracted x-ray intensity function; LPS, lateral phase separation; r^*, z^*, relevant reciprocal space coordinates; SR, sarcoplasmic reticulum; t_h, upper characteristic temperature for lipid lateral phase separation; 2θ, Bragg diffraction angle.

0006-3495/90/07/205/13 $2.00

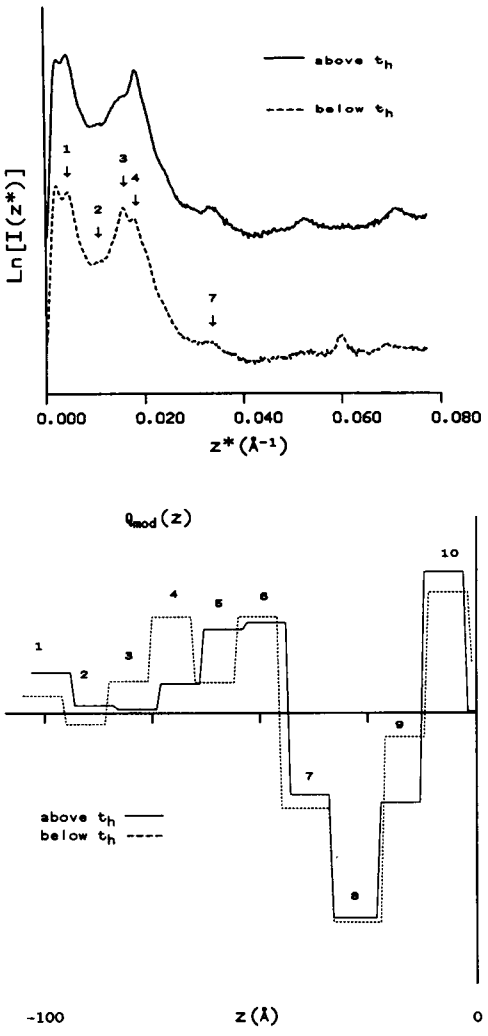

FIGURE 1 (*A*) Typical lamellar diffraction $I(z^*)$ for temperatures above and below t_h for LPS from partially dehydrated (88% relative humidity), oriented multilayers of SR vesicles at ~100 μM [Mg^{+2}]. The numbered arrows indicate the approximate positions of lamellar Bragg orders for the disordered multilayer lattice. Diffraction maxima at higher values of z^* arise as a result from the unsampled unit cell profile structure factor. (*B*) Step-function electron density models of the SR membrane profile, corresponding to continuous electron density profiles (13 Å resolution) calculated directly from the lamellar intensity functions shown in Fig. 1 *A*. Changes occur throughout the membrane profile including the region of the membrane outside the lipid bilayer (steps 1–5) containing the headpiece of the Ca^{+2} ATPase. See reference 3 for details.

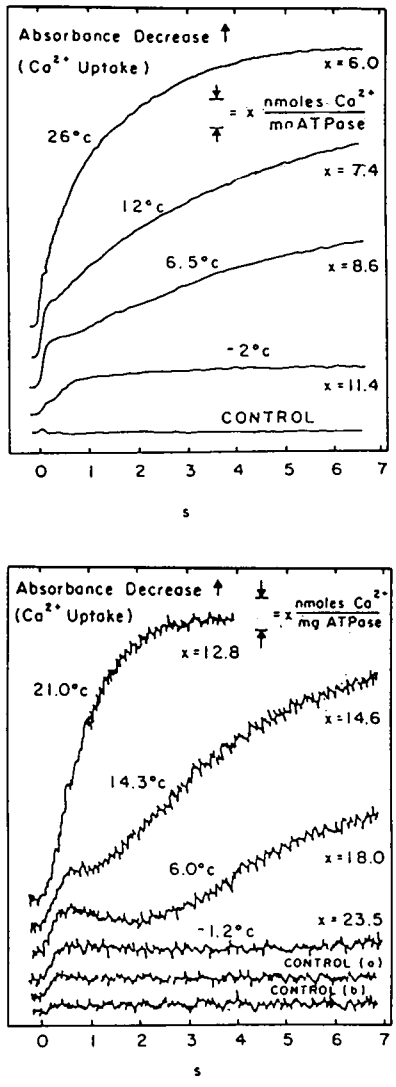

FIGURE 2 Typical Ca^{+2} uptake kinetics for SR vesicular dispersions (*A*), and oriented multilayers (*B*), as a function of temperature. Two distinct, temperature dependent kinetic phases of Ca^{+2} uptake can be observed. The most obvious difference between the results obtained for dispersions and multilayers at equivalent temperature is the duration of the plateau (corresponding to transient trapping of Ca^{+2}ATPase in its first phosphorylated conformation, $E_1 \sim P$) after the initial fast phase and before the second, slow phase. See reference 4 for details.

include a study of the effect of water content, and it is a well established fact that hydration profoundly affects the structure and physical state of phospholipids (5, 6). Furthermore, this previous work could not establish a causal relationship between the observed LPS and the changes observed in the structure and functionality of the Ca^{+2}ATPase. Therefore, it appeared that through a comparative study of the LPS behavior in the intact SR membrane and in bilayers of isolated SR lipids (in the absence of protein), some insight could be gained concerning the role that the lipids, the Ca^{+2}ATPase protein, and lipid-protein interactions play in the behavior of the intact membrane.

In this paper we report the results of our study of the effect of temperature, [Mg^{+2}], and water content on the lipid LPS behavior in bilayers of isolated SR lipids as compared with those for the intact SR membrane, and

discuss possible implications based on our results concerning the effect of protein-lipid interactions on the Ca^{+2} transport function of the Ca^{+2}ATPase.

METHODS

Preparation of SR membranes and isolated SR lipids

Vesicular dispersions of SR membranes were prepared from albino rabbit hind leg muscle (7). The SR preparation was purified by sucrose density gradient centrifugation as described previously (8). Purified vesicles were stored at −70°C, suspended in a buffer (pH 6.85) that contained 100 mM KCl, 2 mM Trisma-maleate, and 10 mM $MgCl_2$, (or no Mg^{+2} salt for the low $[Mg^{+2}]$ studies). Typical concentrations for these SR dispersions were ~10 mg of protein/mL. For the x-ray diffraction experiments, oriented multilayers of SR vesicles were prepared as described previously (9). Concentrated vesicular dispersions, suitable for x-ray diffraction studies were prepared by placing a small volume (~40 μL) of the purified SR dispersion inside an x-ray glass capillary tube (diam 1.5 mm), and centrifuging it at 10,000 *g* for 90 min in a plastic cell designed to support the fragile capillary tubes.

SR lipids were isolated from the purified SR membrane vesicular dispersions after a somewhat simplified version of a standard protocol (10). After the final lipid extract in chloroform-methanol was obtained, the solvent was evaporated to dryness under a stream of nitrogen, the lipids were resuspended in the same buffer used for the SR vesicular dispersions, and were stored under nitrogen at −20°C. The isolated lipids were analyzed by two-dimensional thin layer chromatography (11), and the composition of the SR lipid extract agrees with what has been reported previously (12), namely, ~68% phosphatidyl choline, ~16% phophatidyl ethanolamine, ~9% phosphatidyl inositol, ~2% phosphatidyl serine, and ~2% sphingomyelin (the lipid extracts also contained a small amount of cholesterol and other unidentified neutral lipids). For x-ray diffraction studies, the aqueous lipid dispersions were thawed and briefly sonicated, and then used to prepare concentrated vesicular dispersions or oriented multilayers of partially dehydrated vesicles.

X-Ray diffraction experiments

For the x-ray diffraction experiments a GX-13 rotating anode x-ray generator (Marconi Avionics, Ltd., Borenhamwood, England) was used to produce an x-ray beam (Cu $K_{\alpha 1}$) that was line-focused via Frank optics (13) with a 20-cm long Ni-coated quartz mirror, and further focused to a point (65 cm away from the specimen) with a cylindrically bent, asymmetrically cut Ge (111) monochromator crystal. Diffraction patterns were recorded with a two-dimensional, position-sensitive proportional counter (Nicolet Instruments Co., Madison, WI) interfaced to a dedicated computer (Cadmus Computer Systems, Inc., Lowell, MA). Different specimen-to-detector distances were used for the experiments. In all cases the doubly convergent x-ray beam cross-section was reduced using both defining- and guard-slits until the direct beam, as seen by the detector, was a point with size limited by the detector's resolution (~800 μm^2). Specimen to detector distances (through He-filled flight tubes) were 36 cm for recording of "low" angle diffraction ($2\theta \leq 10°$; x-ray beam at grazing incidence with respect to the surface of multilayer samples, or in transmission for concentrated vesicular dispersion samples), and 5.6 cm for recording of "high" angle diffraction ($2\theta \leq 45°$; in transmission). For some experiments, both high and low angle diffraction data from the same multilayer sample were collected. In those cases, the multilayers were mounted such that a simple rotation allowed the recording of both types of diffraction with a minimum rearrangement of the remainder of the experimental set-up.

All samples were mounted in a temperature-controlled specimen chamber. During the x-ray experiment the temperature was scanned after a procedure analogous to that described before (3). The water content in the multilayer samples (prepared from either SR membranes or isolated SR lipids) was controlled (under sealed conditions) via the use of saturated salt solutions, or using a steady flow of moist He (equilibrated with a saturated salt solution or water). To study the effect of the degree of hydration on the LPS behavior of intact SR membranes and bilayers of isolated membrane lipids, wet samples, sedimented on aluminum foil and mounted in a special support, were placed in the specimen chamber. "Low" angle (at grazing incidence) and "high" angle (in transmission) diffraction patterns were collected as the samples evolved through the partial dehydration process, and eventually formed oriented multilayers of stacked, flattened vesicles at equilibrium. In the case of diffraction patterns recorded from samples with relatively high water content (such as concentrated vesicular dispersions or wet multilayers), scattering from the buffer in which the sample was prepared was recorded. The scattering from the buffer was, in some cases, properly scaled and subtracted from the diffraction patterns to facilitate their interpretation. All the results reported here concerning the effect of degree of hydration on lipid LPS, as well as the conclusions that follow from them, depend only on relative changes in water content. Absolute water contents are not reported in every case, but the range studied included from the very high water content in "concentrated" vesicular dispersions and "wet" multilayers (~80% w/w), to the relatively low water content (~25–30% w/w) in partially dehydrated SR multilayers.

All two-dimensional diffraction patterns were corrected using a two-dimensional correction algorithm to compensate for nonuniformities in detector sensitivity. After correction, the patterns were integrated to reduce them to one-dimensional functions used for further analysis. In the case of lamellar diffraction patterns, obtained at grazing incidence from multilayer samples formed by stacked flattened vesicles and showing a significant degree of orientation, an angular integration algorithm was used to integrate the intensity of the arc-shaped lamellar reflections over the mosaic spread (layer misorientation) of the sample. This resulted in one-dimensional lamellar intensity functions $I(r^* = 0, z^*)$, where r^* and z^* are reciprocal space coordinates for the cylindrically symmetric multilayers (14). In the case of transmission diffraction patterns with total angular symmetry (such as those arising from concentrated vesicular dispersion samples, or equatorial diffraction from oriented multilayers with the x-ray beam incident normal to the layer planes), the symmetric patterns were angularly integrated over 360° to obtain one-dimensional intensity functions $I(r^*)$ and $I(r^*, z^* = 0)$, respectively (14). All the resulting one-dimensional data were transfered to a VAX 11-750 computer (Digital Equipment Corp., Westboro, MA) used for further analysis.

RESULTS AND ANALYSIS

Intact SR membranes

Vesicular dispersions of SR: temperature and $[Mg^{+2}]$ dependence of lipid chain diffraction at high water content

Highly concentrated vesicular dispersions of SR membranes (prepared by sedimenting a dispersion of SR vesicles inside an x-ray glass capillary tube) were used to study the dependence on temperature (between −2° and 18°C) and $[Mg^{+2}]$ (~40 μM and 10 mM Mg^{+2}) of the

diffraction arising from the packing of lipid alkyl chains in the plane of the membrane. For these spherically symmetric samples, broad, angularly symmetric diffracted intensity was observed for $10° \leq 2\theta \leq 50°$. At higher diffraction angle, the patterns are dominated by the scattering from the buffer in which the SR vesicles were suspended. Diffraction from the lipid chain packing in the membrane plane can be observed only as a weak, broad ring at somewhat lower diffraction angle riding on the broader, much more intense water scattering peak. Scattering from the buffer was recorded by lowering the sample so that only the buffer remaining on top of the sedimented vesicles intersected the x-ray beam. By substracting this background scattering (after proper scaling), it is possible to observe a pattern consisting of two broad, ring-like reflections. Background-substracted one-dimensional intensity functions $I_c(r^*)$ obtained by angular integration over 360° of two-dimensional patterns obtained from a typical sample with low [Mg^{+2}] (~40 μM), equilibrated at several different temperatures, are shown in Fig. 3. Identical results were obtained for samples with higher (10 mM) [Mg^{+2}]. In these patterns, the first peak at smaller r^* corresponds to a mean Bragg spacing of $\sim 1/10$ $Å^{-1}$ and arises from the packing of α-helices in the protein (15). The second, broader peak at larger r^* corresponds to a mean Bragg spacing of $\sim 1/4.5$ $Å^{-1}$ and arises from the packing of lipid chains in the membrane plane. Melted lipid chains with a highly disordered liquid-like distribution in the membrane plane will give rise to a broad, symmetric peak, such as that observed in Fig. 3 *A*.

At the relatively high water content characteristic of these "concentrated" vesicular dispersion samples, variations in temperature within the range studied do not induce significant changes in the diffraction arising from the packing of the lipid chains in the membrane plane. The chains remain in a smectic, liquid-crystalline state. None of the diffraction patterns show evidence of the lipid

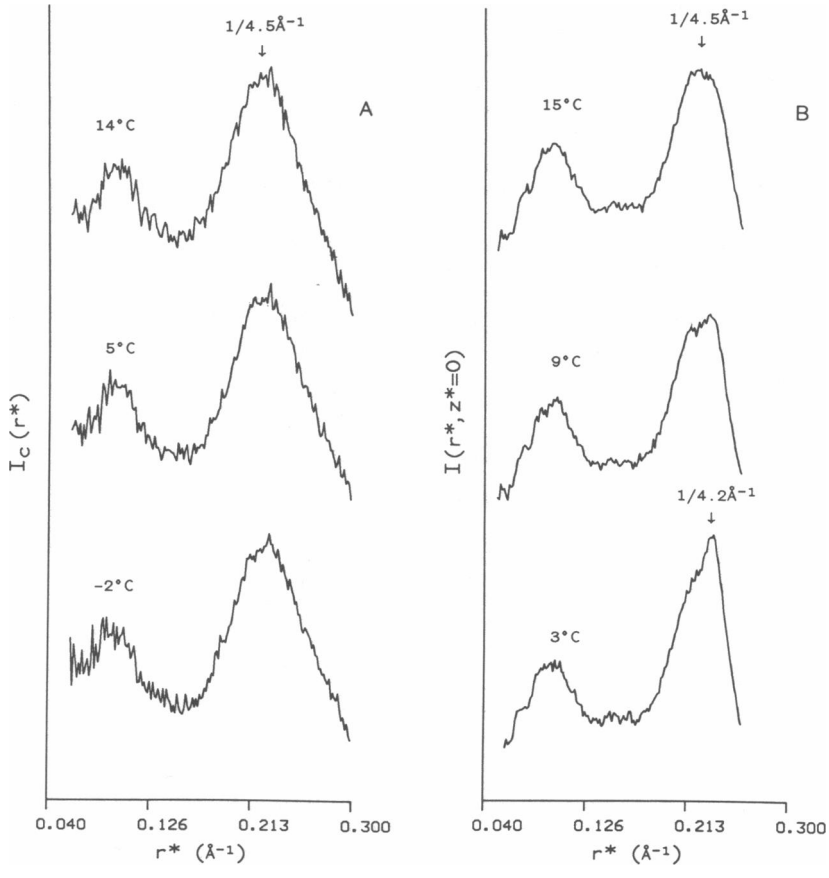

FIGURE 3 (*A*) One-dimensional intensity functions $I_c(r^*)$ obtained from high angle diffraction patterns arising from a concentrated dispersion of unilamellar SR vesicles at low [Mg^{+2}] (~40 μM) as a function of temperature. See text for details. (*B*) One-dimensional intensity functions $I_c(r^*, z^* = 0)$ obtained from high angle, equatorial diffraction patterns arising from a partially dehydrated (88% relative humidity), oriented multilayer of flattened SR vesicles at low [Mg^{+2}] (~100 μM) as a function of temperature. See text for details.

LPS that would result from the presence of domains of "frozen" lipid chains arranged in a hexagonal lattice in the plane of the membrane (1). The presence of frozen lipid chains would give rise to a sharper reflection with a larger mean radius, corresponding to a Bragg spacing closer to $\sim 1/4.2$ Å^{-1}. To contrast these results with what would be observed for a sample where lipid LPS had occurred, the patterns presented in Fig. 3 *A* can be compared with those presented in Fig. 3 *B*, that correspond to equatorial diffraction patterns from a partially dehydrated, oriented SR multilayer, where the water content is significantly lower. In this case, a significant degree of LPS is observed at lower temperature, as evidenced by the marked asymmetry of the lipid chain diffraction peak due to the presence of a sharp peak (corresponding to a Bragg spacing of $\sim 1/4.2$ Å^{-1}), arising from two-dimensionally crystalline domains of "frozen," lateral phase separated lipid chains.

Oriented multilayers of SR: temperature and [Mg^{+2}] dependence of LPS at low water content

As we reported previously (2, 3), for partially dehydrated, oriented SR multilayers, lateral phase separation of the membrane lipids is observed (see Fig. 3 *B*). The upper characteristic temperature for LPS, t_h, shows a clear dependence on the [Mg^{+2}]. At high [Mg^{+2}] ($\sim$25 mM), t_h for LPS of the membrane lipids is $\sim$2°–3°C, and for low [Mg^{+2}] ($\sim$100 μM), t_h has a value of $\sim$8°–10°C.

Oriented multilayers of SR: LPS as a function of degree of hydration at constant $T < t_h$

Because the preceeding results had indicated that LPS of the SR membrane lipids is observed at relatively low water content (partially dehydrated multilayers), and that LPS does not occur in SR vesicular dispersions (relatively high water content), it seemed important to study the LPS behavior as a function of water content in the SR samples. This was achieved by following the evolution of both lamellar and equatorial diffraction from SR samples as they were partially dehydrated at a constant temperature, lower than that previously observed to correspond to the upper characteristic temperature (t_h) for LPS of the membrane lipids (2, 3) at relatively low water content. The samples, that started as vesicular dispersions, were either equilibrated with a saturated salt solution under sealed conditions, or exposed to a steady flow of moist He at constant relative humidity. In this way, the samples were partially dehydrated until they formed equilibrated, oriented multilayers.

A set of one-dimensional intensity functions obtained by integration of two-dimensional equatorial and lamellar diffraction patterns collected from a sample with progressively lower water content is shown in Fig. 4. During partial dehydration the temperature of the sample was kept constant at 2.2 ± 0.2°C, and the [Mg^{+2}] was $\sim$100 μM (similar results were obtained when the [Mg^{+2}] was higher). Initially (Fig. 4 *B*, time = 00:42 h), the low angle diffraction ($2\theta \leq 10°$) is rather featureless, and resembles that from a spherically symmetric dispersion of swollen unilamellar vesicles (16). The higher angle diffraction ($10° \leq 2\theta \leq 50°$) shows a very intense, broad water peak, with a small shoulder on the low angle side, corresponding to the lipid chain diffraction (Fig. 4 *A*, time = 00:14 h). Subtraction of the water scattering, scaled such that the intensity of the remaining water scattering is roughly equivalent to that in the partially dehydrated multilayer, reveals a broad, symmetric lipid chain diffraction peak corresponding to a mean Bragg spacing of $\sim 1/4.5$ Å^{-1} (*dotted line* in Fig. 4 *A*) characteristic of melted lipid chains in a liquid crystalline state (5). As the dehydration progresses, the low angle diffraction shows that the sample starts to show some degree of order and orientation, as the vesicles start to collapse and form stacks (Fig. 4 *B*, time = 02:37 h). During this time the high angle patterns show a progressively weaker water scattering (Fig. 4 *A*, time = 01:33 h). Again, subtraction of the scaled water scattering reveals a lipid chain diffraction peak characteristic of melted lipid chains (*dotted line*). The time at which the bulk water peak virtually disappears coincides with the time when lamellar reflections are first observable in the low angle diffraction pattern. When the lamellar reflections can be distinguished, the lamellar periodicity of the sample can be measured. A General Fourier Synthesis Deconvolution Method of analysis (17) was used to analyze one-dimensional lamellar intensity functions $I_c(r^* = 0, z^*)$ obtained from the original integrated intensity functions $I(r^* = 0, z^*)$ after subtraction of a piece-wise continuous exponential approximation to the lamellar background scattering, and application of a Lorentz correction of z^* (18). This analysis shows that after the lamellar reflections first appear the multilayer sample continues to lose water. There is a significant change in periodicity (15–20% of final periodicity) from the time when the lamellar reflections are first observed, to the time when the sample reaches its final equilibrium periodicity (Fig. 4 *B*, time = 04:38 h), that for our experimental conditions was typically $\sim$190 Å. At this point, the equatorial lipid chain diffraction consists of an asymmetric peak, with a sharp component corresponding to a mean Bragg spacing of $\sim 1/4.2$ Å^{-1} superimposed on the broad chain diffraction peak at $\sim 1/4.5$ Å^{-1} (Fig. 4 *A*, time = 04:19 h). This is an indication of the presence of domains of "frozen," lateral phase separated lipid chains occurring over the membrane plane (5).

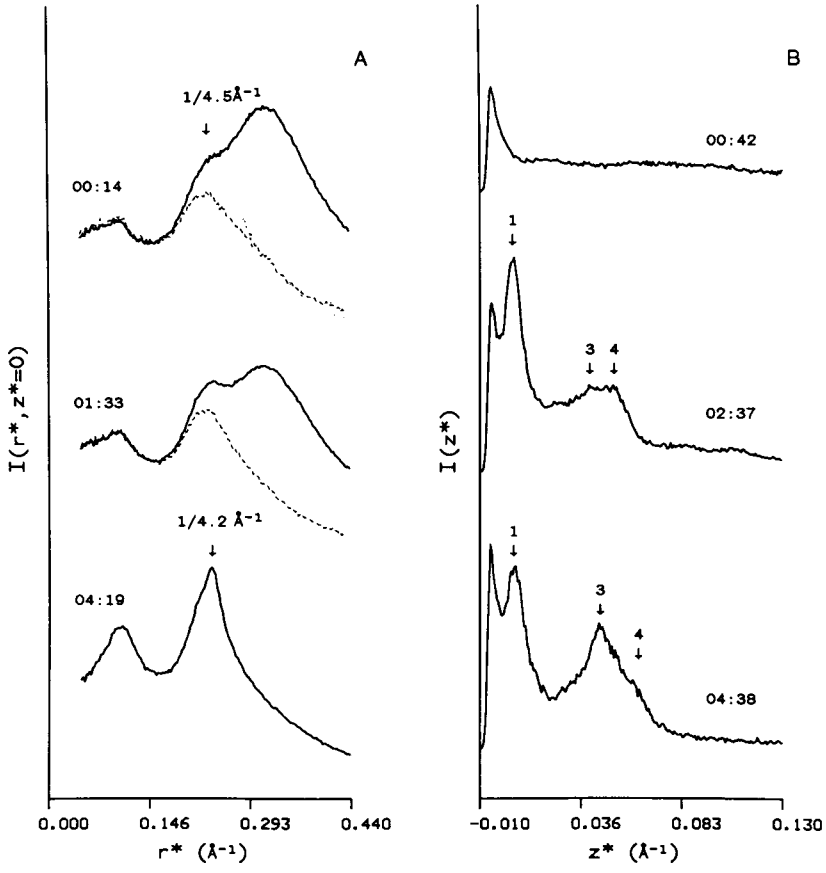

FIGURE 4 (*A*) One-dimensional intensity functions $I(r^*, z^* = 0)$ obtained from high angle, equatorial diffraction patterns arising from an ultracentrifuged pellet of SR vesicles collected while the pellet was undergoing partial dehydration in a sealed cannister. The relative humidity was controlled using a saturated KCl solution (relative humidity 88% at 0°C), and the temperature of the sample was maintained at 2.5°C. The times in the figure indicate the time at which data collection was initiated (the beginning of partial dehydration was taken as time 00:00, and all patterns correspond to 600 s of data collection). The broader, more intense peak in the top (*solid line*) pattern (00:14 h), arises from the bulk water present in the wet sample. After subtraction of the water scattering background, the diffraction arising from lipid chain packing in the plane of the membrane can be observed more easily (*dotted line pattern*). See text for details. (*B*) One-dimensional intensity functions $I(z^*)$, obtained from the corresponding lamellar diffraction arising from the same sample from which the equatorial diffraction patterns in Fig. 4 *A* were collected. See text for details.

It is interesting to note that when the lamellar reflections first appear (Fig. 4 *B*, time = 02:37 h), the third and fourth orders have comparable intenssties (we have found previously that this is always the case for partially dehydrated multilayers that do not present any LPS) (2, 3). Examination of the equatorial diffraction patterns in Fig. 4 *A* indicates that at this time only a broad, symmetric equatorial lipid chain diffraction peak, indicative of the absence of LPS is present. At this stage, the samples have lamellar periodicities of ~220–230 Å. As the sample loses more water the equatorial lipid chain diffraction shows at first an asymmetry in the shape of the original broad peak, and then the appearance of a sharper peak on the high angle side of the original broad peak. The sharper peak (centered at $\sim 1/4.2$ Å^{-1}) arises from ordered domains of frozen lipid chains packed in a hexagonal lattice in the membrane plane, and coinciding with the appearance of diffraction from the frozen lipid chains, the lamellar intensity functions show a change in the ratio of the intensity of the third- and fourth-order reflections (the third-order reflection becomes stronger than the fourth-order), a phenomenon that we have always found to occur as the membrane lipids start to phase separate (3).

To summarize, for these SR multilayer samples equilibrated at temperatures below the t_h value for LPS of the membrane lipids, no LPS is observed as long as the sample has a relatively high water content. This agrees with our observation of no LPS in concentrated dispersions of SR vesicles. As the samples evolve through the process of partial dehydration, the vesicles eventually collapse and stack; the membrane lipids start to phase separate only after the water content in the samples is reduced further.

Studies on bilayers of isolated SR lipids

Vesicular dispersions of isolated SR lipids: temperature and [Mg^{+2}] dependence of lipid chain diffraction at high water content

In general, the results obtained for concentrated vesicular dispersions of isolated SR lipids are similar to the results obtained for vesicular dispersions of intact SR membranes. Integrated intensity functions, $I_c(r^*)$, obtained after subtraction of the scaled water scattering for an isolated lipid vesicular dispersion sample with low [Mg^{+2}] (~40 μM) at 0° and 20°C are shown in Fig. 5 *A*. As observed for intact SR membrane vesicles, at the relatively high water content that characterizes these vesicular dispersions, variations in temperature within the range studied do not induce significant changes in the diffraction from the lipid chain packing in the bilayer plane. There is no indication in the diffraction patterns of the occurrence of lipid LPS. This is true for both of the [Mg^{+2}] studied. Notice that the lower angle peak arising from the protein α-helices is of course absent in the patterns obtained from vesicular dispersions of isolated lipids.

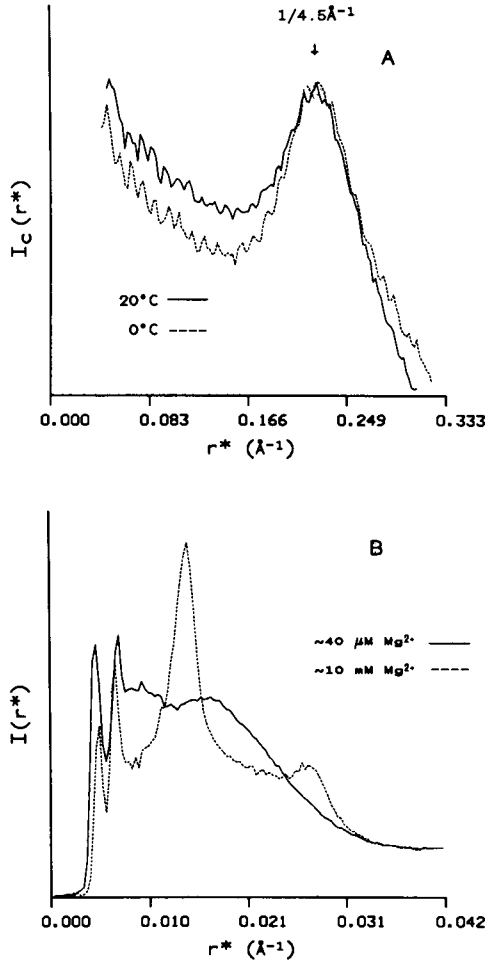

FIGURE 5 (*A*) One-dimensional intensity functions $I_c(r^*)$ obtained from high angle diffraction patterns arising from a concentrated dispersion of vesicles of isolated SR lipids. Both intensity functions arise from the same sample ([Mg^{+2}] ~40 μM), equilibrated at the temperature indicated. See text for details. (*B*) Intensity functions $I(r^*)$ corresponding to the lower angle diffraction from a concentrated dispersion of vesicles of isolated SR lipids at two different [Mg^{+2}]. See text for details.

Whereas the lipid chain diffraction does not show any significant dependence on the [Mg^{+2}], the same is not true for the "low angle" ($2\theta \leq 10°$) diffraction. Examination of the two-dimensional diffraction patterns indicates that they are angularly symmetric over 360°, as would be expected from vesicular dispersions. However, for high [Mg^{+2}], a sharp, intense ring corresponding to a Bragg spacing of ~69 Å can be observed. A second-order reflection corresponding to the same spacing is also observed. This is illustrated in Fig. 5 *B*, that shows integrated intensity functions $I(r^*)$ for vesicular dispersion samples at high and low [Mg^{+2}]. The sharp peak in the high [Mg^{+2}] pattern arises from the presence of a significant concentration of multilamellar ("onion-skin") vesicles. This contrasts with what was found for lipid vesicular dispersions at low [Mg^{+2}] (~40 μM), where the totality of the lipids are present in the form of unilamellar vesicles, (or possibly swollen multilamellar vesicles with large and/or irregular interbilayer water spaces), as indicated by the shape of the integrated intensity function. The presence of multilamellar vesicles in the high [Mg^{+2}] samples could not be prevented by sonication for brief periods of time (<3 min), whereas for the low [Mg^{+2}] samples, the lipids always formed unilamellar vesicles, independently of whether the samples were sonicated or not. As for the temperature dependence of the low angle diffraction patterns, only slight changes were observed.

Oriented multilayers of isolated SR lipids: temperature and [Mg^{+2}] dependence of LPS at low water content

To study the temperature dependence of the LPS behavior for multilayers of isolated SR lipids, samples were partially dehydrated and equilibrated at a temperature higher than the corresponding t_h value for LPS for the intact SR membrane under similar conditions. Then, the effect of temperature on the lamellar and equatorial diffraction from these samples was studied after a protocol analogous to that used previously in the case of SR membrane multilayers (3). A set of one-dimensional intensity functions $I(r^*, z^* = 0)$ obtained by angular integration of background scattering-corrected equatorial

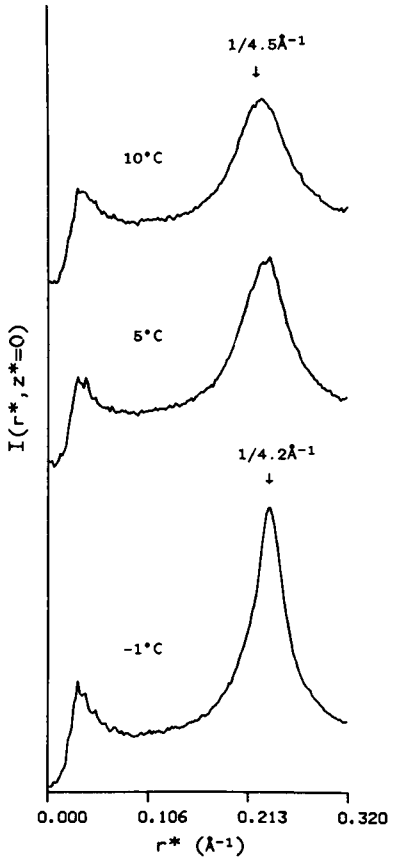

FIGURE 6 One-dimensional intensity functions $I(r^*, z^* = 0)$ obtained from high angle, equatorial diffraction patterns arising from a partially dehydrated multilayer of isolated SR lipids. See text for details.

diffraction patterns from a typical isolated lipid multilayer as a function of temperature is shown in Fig. 6. As can be seen from the figure, the equatorial diffraction at relatively high temperatures shows one symmetric, broad peak, corresponding to a mean Bragg spacing of $\sim 1/4.5$ $Å^{-1}$. At lower temperatures, an additional sharper peak, corresponding to a mean Bragg spacing of $\sim 1/4.2$ $Å^{-1}$ appears. This is an indication of the presence of two-dimensionally crystalline domains of frozen lipid chains over the bilayer plane. For both high and low $[Mg^{+2}]$, the sharper peak indicative of the presence of lateral phase separated lipids first appears at a temperature of 6 ± 1°C. No significant difference in the value of t_h was found for the two $[Mg^{+2}]$ studied.

We had previously found that the degree of lipid LPS observed for SR membrane multilayers upon decreasing the temperature below t_h was dependent on the $[Mg^{+2}]$: LPS was much more extensive at low $[Mg^{+2}]$ (2, 3). Comparison of the patterns shown in Fig. 6 with those obtained from intact SR membrane multilayers under similar conditions, indicates that for the isolated lipid samples, the extent of LPS shows no $[Mg^{+2}]$ dependence, and is much larger than that observed for the intact SR membrane samples under any of the conditions studied.

The lamellar diffraction patterns that correspond to the equatorial patterns shown in Fig. 6 are not presented, but they indicate that initially (before the onset of LPS), the lipids in the multilayer form a single lamellar phase. The first four reflections from this lamellar phase (with a periodicity of ~59 Å) were recorded. Upon decreasing the temperature below t_h, a second lamellar phase forms. This new lamellar phase has a periodicity of ~62 Å. Our observations concerning this phenomenon are presented in more detail in the following section.

Oriented multilayers of isolated SR lipids: LPS as a function of degree of hydration at constant $T < t_h$

As indicated in the preceding sections, similarly to what was observed for lipids in the intact SR membrane, bilayers of isolated SR lipids only show LPS at relatively low water contents. Samples with relatively high water content (such as vesicular dispersions) show no LPS under the temperature and $[Mg^{+2}]$ conditions examined. To obtain more information about the behavior of the isolated SR lipid bilayers, the dependence of their LPS behavior on the degree of hydration was studied.

During partial dehydration of a sample of isolated lipids, x-ray reflections from a single lamellar phase are observed as soon as the sample has lost enough water for the lipid vesicles to start to collapse and stack to form a multilayer. Up to four reflections from this lamellar phase were recorded. The first-order reflection is significantly stronger than the higher-order ones, whose intensity depends strongly on the water content in the sample. In multilayers with relatively high water content the second-, third-, and fourth-order reflections have comparable intensities, but as the water content in the multilayer decreases, the second- and third-order reflections become weaker. Much of what occurs in the multilayer is reflected in the behavior of the strong first-order lamellar reflection. This is illustrated in Fig. 7, which shows the low angle region of the lamellar diffraction patterns obtained from a multilayer of isolated SR lipids during partial dehydration at −3.5°C (patterns *a* through *f*), followed by reequilibration at 12°C (patterns *g* and *h*, other patterns collected during reequilibration to high temperature are not shown). Initially, the first-order lamellar reflection gains in intensity, and progressively moves to higher angle (Fig. 7, *a* and *b*) as the sample becomes better ordered and the lamellar periodicity becomes smaller due to decreasing water content in the

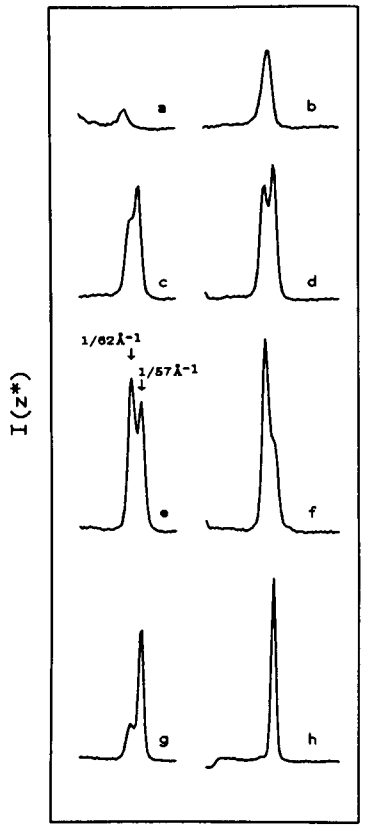

FIGURE 7 One-dimensional intensity functions $I(z^*)$ obtained from the low angle lamellar diffraction patterns arising from an oriented multilayer of isolated SR lipids collected while the multilayer was partially dehydrated at a constant temperature of -3.5°C (patterns *a* through *f*). The diffraction patterns included more reflections at larger z^*, but this figure shows only the low angle portion of the collected patterns. After the sample had reached its equilibrium state of partial dehydration, the temperature was rapidly increased to 12°C (patterns *g* and *h*). See text and Fig. 8 for details.

sample. The lamellar spacing changes from ~69 Å (when the reflection first appears), to a final value of ~57 Å. Examination of the high angle ($2\theta \leq 45°$) equatorial diffraction patterns recorded during this time period shows that the intensity of the water scattering on the high angle side of the lipid chain diffraction peak (which up to this point shows no evidence of LPS) progressively decreases. After the water scattering peak has virtually disappeared and the lamellar periodicity of the sample (as judged by the z^* position of the first-order lamellar reflection in the lamellar diffraction patterns) has decreased to ~57 Å, the equatorial lipid chain diffraction patterns show evidence of LPS (a sharp peak centered at $\sim 1/4.2$ Å^{-1} appears on the high angle side of the original broad peak centered at $\sim 1/4.5$ Å^{-1}), and in the lamellar diffraction patterns, two additional reflections can be observed on the lamellar (meridional) axis. The use of an x-ray beam that was point-focused on the detector, and the low mosaic spread (good layer–layer orientation) shown by the samples allow us to conclude that the new reflections are indeed on the lamellar axis, and are not projections of off-axis reflections coming from a nonlamellar lipid phase (19). These two reflections correspond to the first and fourth orders of a second lamellar phase, with a periodicity of ~62 Å. In Fig. 7 (*c* through *g*), the first-order reflection from this new lamellar phase can be seen on the low angle side of the originally present first-order lamellar reflection. The second- and third-order reflections from this new lamellar phase were not observed. The larger periodicity shown by the lamellar phase that appears at relatively low water content (after partial dehydration), the ratio of intensities of the lamellar reflections from this phase (the first- and fourth-orders are much stronger than the second- and third-orders), and the changes observed in the equatorial lipid chain diffraction patterns, lead us to conclude that this new lamellar phase consists of stacked domains of "frozen" lipid chains. Coexistence of two lamellar phases in a biological membrane system had been observed before: hypertonic saline conditions, or exposure to dimethylsulfoxide cause the appearance of a "contracted" lamellar phase in nerve myelin samples (20, 21). As in all previous circumstances (for both intact SR membranes and bilayers of isolated SR lipids), increasing the temperature of the sample rapidly reverses the lipid LPS, which in this case is manifested by a sharp decrease of the intensity of the reflections arising from the higher periodicity lamellar phase, followed by their eventual disappearance, as well as by the disappearance of the $\sim 1/4.2$ Å^{-1} reflection from the equatorial lipid chain diffraction patterns. Both the appearance and disappearance of the reflections arising from the lamellar phase formed by the "frozen" lipid chains is rather sudden. This can be better appreciated by looking at Fig. 8, where the ratio of the intensity of the first-order lamellar reflection arising from the "frozen" chains to the intensity of the first-order lamellar reflection coming from the melted chains as a function of time is presented. The rapid reversibility of the observed phase separation suggests that the two lamellar phases that are present at low temperature and low water content may be topologically connected.

DISCUSSION

In this section we will summarize our results concerning the effect of temperature, [Mg^{+2}], and degree of hydration on lipid lateral phase separation in the intact SR membrane and in isolated SR lipid bilayers. We will also

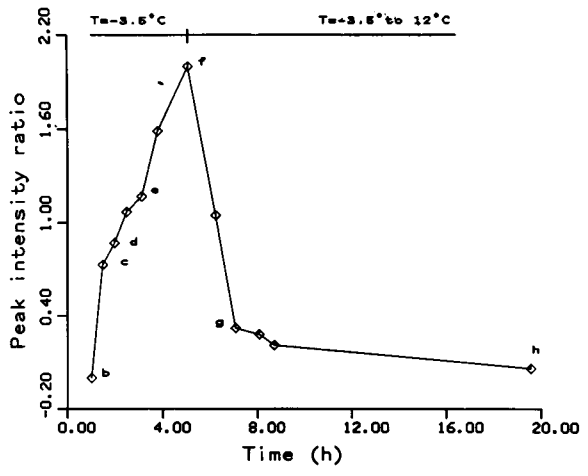

FIGURE 8 Ratio of the peak intensities of the two, first-order lamellar reflections in the diffraction patterns shown in Fig. 7. The values are plotted as the ratio of the intensity of the lower angle reflection to the intensity of the higher angle reflection. See text for discussion.

discuss the significance of these results with regard to the correlations between membrane lipid behavior and the structure and functionality of the Ca^{+2}ATPase.

LPS in the SR membrane and isolated SR lipid bilayers: effect of temperature, [Mg^{+2}], and degree of hydration

Given the high protein concentration in the native SR membrane (lipid/protein mole ratio ~115/1) (22), it is somewhat surprising that bilayers of lipids isolated from the membrane show a LPS behavior that does not differ significantly from their behavior in the intact membrane. In general, the only significant difference that we found between LPS behavior in the isolated lipid bilayers and in the intact membrane is that LPS behavior in the isolated lipid bilayers does not seem to be as sensitive to changes in [Mg^{+2}]. Under similar conditions, LPS is much more extensive in isolated lipid bilayers, and no significant dependence of either the extent of LPS or the value of t_h on [Mg^{+2}] is observed. In contrast, in the intact membrane the extent of LPS increases and the value of t_h is significantly higher at low [Mg^{+2}] (3). From our results it is not possible to establish the reason for the difference in the LPS behavior of the membrane and the isolated lipid bilayers. The asymmetry present in the lipid bilayer of the native membrane (12, 22), that is no longer present in the isolated lipid bilayer samples, could be responsible for the difference in the behavior of the two systems. In addition, in the case of the intact membrane, the [Mg^{+2}] effect may be modulated by either the Ca^{+2}ATPase or characteristics of the lipid-protein interface that are of course absent in isolated lipid bilayers.

We found water concentration to be a very important factor in the lipid LPS behavior of both the intact membrane and bilayers of its isolated lipids. This is as expected. For example, Luzzati and co-workers reported as part of their extensive investigation of the phase diagram of water-lipid phases that for many lipids, the formation of ordered β-phases (with all trans-, frozen lipid chains packed in a hexagonal lattice in the plane of the bilayer) is only observed at low water contents (5). For the SR membrane and isolated SR lipid bilayer samples, we observed no LPS (in the range of temperature and [Mg^{+2}] studied) under conditions where the water content is relatively high (e.g., "wet" multilayers or vesicular dispersions). Previous studies of LPS in the SR membrane have, for the most part, failed to detect the occurrence of extensive LPS in the system. Only a very small amount of lateral phase separation was observed in x-ray diffraction studies of SR and its isolated lipids by Davis et. al. (23), presumably, due to high water content in the samples utilized.

Results from our studies of the effect of [Mg^{+2}] on the profile structure of the SR membrane (3) have provided evidence that indicates that water content may also play a role in mediating this [Mg^{+2}] effect. By comparing electron density strip models of the SR membrane profile at different [Mg^{+2}] and equivalent "high" temperatures above their respective [Mg^{+2}]-dependent value of t_h, we found that a decrease in [Mg^{+2}] causes changes in the structure of the membrane lipids even at temperatures well above t_h. At low [Mg^{+2}] (~100 μM), the separation between lipid polar head groups across the membrane profile is larger, and the position of the terminal methyl groups of the lipid alkyl chains is much better defined. These changes in lipid structure induced by decreasing [Mg^{+2}] are indicative of a progressive decrease in lipid chain flexibility, and are analogous to the changes induced in lipid bilayers, at temperatures above t_h, by decreasing water content (6). At temperatures below t_h, we observed that the dependence on [Mg^{+2}] of LPS in the SR membrane cannot be explained in terms of neutralization of repulsive interactions between charged polar head groups by metallic cations. Based on the results from NMR studies of the effect of divalent cation concentration on the LPS behavior of lipid mixtures (24), we suggested (3) that the degree of hydration of the phospholipid polar head groups was affected by the concentration of highly hydrated metal cations such as Mg^{+2}, thereby explaining the [Mg^{+2}] dependence of the LPS behavior observed in the intact membrane at relatively low water contents. These results lead us to believe that the effect of

[Mg^{+2}] on the structure of the SR membrane lipids is mediated (at temperatures both above and below t_h) by [Mg^{+2}]-dependent changes in water activity.

Lipid-protein interactions: correlations between lipid phase behavior and structure and functionality of the Ca^{+2}ATPase

It is relevant to relate the results of this study to the results of our earlier measurements of Ca^{+2}ATPase functionality, evaluated in terms of the kinetics of ATP-induced Ca^{+2} uptake in vesicular dispersions and partially dehydrated, oriented multilayers of SR vesicles (4, 3). Our studies of the kinetics of Ca^{+2} uptake indicated that the behavior of vesicular dispersions and multilayer samples is in general very similar in regard to their temperature dependence. One important difference, however, is the fact that, at the same temperature, the lifetime of the first phosphorylated enzyme intermediate ($E_1 \sim P$) in the Ca^{+2} transport cycle of the Ca^{+2}ATPase protein is always significantly greater in multilayer samples than in vesicular dispersions. In particular, for partially dehydrated multilayers, the lifetime of the $E_1 \sim P$ intermediate was found to be significantly extended at temperatures below the temperature corresponding to the [Mg^{+2}]-dependent t_h for LPS of the membrane lipids (2–4). Also, the transient trapping of the Ca^{+2}ATPase in the $E_1 \sim P$ conformation is most effective in the case of multilayer samples partially dehydrated at temperatures below t_h. Because we found evidence of lipid LPS only at relatively low water contents, it seems that the effects of water content on lipid LPS behavior in the membrane and on the lifetime (or transient trapping) of the $E_1 \sim P$ intermediate are correlated.

The preceeding observations support our conclusion concerning the functional significance of the changes induced in the Ca^{+2}ATPase profile structure by LPS of the membrane lipids (2, 3; see also Figs. 1 and 2 in this paper). The pronounced, correlated hysterisis effects observed as a function of temperature and water content in LPS behavior, Ca^{+2}ATPase structural changes, and $E_1 \sim P$ lifetime, are indicative of the strong coupling among these three phenomena. Such hysterisis effects might be explained as follows. If an SR multilayer sample (such as the ones that we have used for our Ca^{+2} uptake and x-ray diffraction experiments) were partially dehydrated at temperatures above t_h and later equilibrated at a temperature below t_h, the decrease in temperature would cause LPS of the membrane lipids, but due to the relatively low water content of the sample, the lipid chain flexibility (6) and therefore presumably the lateral mobility (i.e., translational freedom in the membrane plane) of the lipid molecules would be reduced. Hence, the degree of LPS, and therefore the changes in the structure of the Ca^{+2}ATPase and the resulting increase in the lifetime of the $E_1 \sim P$ conformation, would not be as extensive. Conversely, if a multilayer were partially dehydrated at temperatures below t_h, a significant fraction of the lipid chains would "freeze" while the water content and lipid lateral mobility were still relatively high. This would produce a greater degree of LPS, and therefore, more significant changes in the structure of the Ca^{+2}ATPase that would result in a greater extension of $E_1 \sim P$ lifetime.

We therefore believe that the structure of the membrane lipids has a decisive influence on the Ca^{+2} transport function of the Ca^{+2}ATPase. Physico-chemical parameters (such as temperature, [Mg^{+2}], and water content) that affect the Ca^{+2} transport function of the protein, also have an effect on the structure of the membrane lipids that is similar in all cases. A decrease in temperature, [Mg^{+2}], or water content (or any combination of the above), will cause a reduction in the chain flexibility and therefore presumably the intermolecular mobility of the membrane lipids, and at the same time, will slow down the kinetics of Ca^{+2} transport by the Ca^{+2}ATPase. Whereas there has been no previous report specifically concerning the effects of LPS of the SR lipids on the functionality of the Ca^{+2}ATPase, other studies have found correlations between ATPase activity and lipid chain flexibility (25–27), between ATPase activity and lipid chain flexibility and protein rotational mobilities (28, 29), and between Ca^{+2} transport/ATPase activities and lipid bilayer thickness (27–30), and phospholipid intra- and intermolecular mobility (23). These studies on both isolated and reconstituted SR membrane systems have established the existence of relationships between the physical state of the membrane lipids and the functionality of the Ca^{+2}ATPase, but in general have not demonstrated how such relationships arise. It has been proposed, for example, that the physical state of the lipids affects the functionality of the protein through its effect on protein mobility (28, 29), but the results reported have not been sufficient to establish whether the physical state of the lipids is affecting the rotational and thereby lateral mobility of the protein (and therefore influencing hypothetical protein–protein interactions proposed to be essential for protein function), or whether it is affecting protein rotational motions related to induced changes in the conformation (and therefore function) of the protein.

Our studies of the SR membrane profile structure have established the occurrence of large scale changes in the profile structure of the Ca^{+2}ATPase that seem to be essential for the Ca^{+2} transport function of the protein. These structural changes involve the redistribution of a significant fraction of protein mass across the membrane

profile (31–33). Namely, upon phosphorylation of the Ca^{+2}ATPase and formation of $E_1 \sim P$, a net *inward* movement of protein mass from the "headpiece" of the protein, to the inner, nonpolar core of the membrane is observed. Conversely, we have found that the structural changes in the membrane profile caused by the same physico-chemical parameters that induce LPS of the membrane lipids and thereby slow the formation and extend the lifetime of $E_1 \sim P$ comprise a net *outward* movement of protein mass from the inner nonpolar core of the membrane to the "headpiece" of the protein on the extravesicular membrane surface (2, 3). These latter structural changes are therefore *opposite* to those that we have found to occur upon phosphorylation of the Ca^{+2}ATPase. In both cases, the mass movement is of similar magnitude, and involves 10–15% of the total protein mass of the Ca^{+2}ATPase. The membrane lipids can either respond and accommodate these changes in protein structure (as for $T > t_h$, high $[Mg^{+2}]$ and/or high water activity) or conversely, can hinder them (as for $T < t_h$, low $[Mg^{+2}]$ and/or low water activity).

We therefore propose that the effect of the physical state of the membrane lipids on the ATP-induced transport of Ca^{+2} by the Ca^{+2}ATPase, is due to changes in phospholipid chain flexibility and lateral molecular mobility and thereby the capacity for lateral compressibility *in each monolayer* of the membrane lipid bilayer. This lateral compressibility allows for protein conformational changes which are essential for transport and involve redistribution of protein mass across the membrane profile. This proposal is independent of the degree of partitioning of the Ca^{+2}ATPase between the solid and fluid phases for $T < t_h$ and provides an explanation for the effects of $[Mg^{+2}]$ and water activity for $T > t_h$. Fox, McConnell, and co-workers used similar arguments to explain the relation observed between breaks in Arrhenius plots for sugar transport in *Escherichia coli*, and the characteristic temperatures for the lateral phase separation observed for the membrane lipids (34, 35).

CONCLUSION

The study of the effects of variations in physico-chemical parameters on the structure and the functionality of a biological system can help to establish the existence of important structure-function correlations in the system. We have characterized the lipid lateral phase separation (LPS) behavior of SR membrane lipids in both the intact membrane and in bilayers of isolated lipids as a function of temperature, $[Mg^{+2}]$, and water content. The LPS behavior in both systems is remarkably similar with respect to its dependence on the parameters examined, and is characteristic of order–disorder transitions for lipid mixtures.

Results from our previous studies of the profile structure of the SR membrane and the kinetics of ATP-induced Ca^{+2} uptake by the SR as a function of the same physico-chemical parameters examined in this report indicated the existence of a transition in the profile structure of the Ca^{+2}ATPase that occurs over a narrow temperature range about t_h, the upper characteristic temperature for LPS of the membrane lipids. According to our results, this structural transition is responsible for slowing the formation, and significantly extending the lifetime of the first phosphorylated intermediate, $E_1 \sim P$ in the Ca^{+2} transport cycle by the SR membrane (2–3). Correlation of these previous findings with the results presented in this report indicates that the LPS behavior observed in the intact SR membrane is a result of the intrinsic behavior of the membrane lipids, and is only weakly influenced by the presence of the Ca^{+2}ATPase. Our results strongly suggest that the intrinsic behavior of the membrane lipids is directly responsible for the large scale structural changes in the Ca^{+2}ATPase profile structure that significantly affect its Ca^{+2} transport function.

We are indebted to Dr. David Chester (Biomolecular Structure Analysis Center, University of Connecticut, Farmington, CT) for determining the composition of the SR isolated lipid extracts used in this study.

This work was supported by National Institutes of Health grant HL-18708 to J. K. Blasie.

Received for publication 7 August 1989 and in final form 4 December 1989.

REFERENCES

1. Shimshick, E., and H. M. McConnell. 1973. Lateral phase separation in phospholipid membranes. *Biochemistry.* 12:2351–2360.
2. Pascolini, D., and J. K. Blasie. 1988. Moderate resolution profile structure of the sarcoplasmic reticulum membrane under low temperature conditions for the transient trapping of $E_1 \sim P$. *Biophys. J.* 54:669–678.
3. Asturias, F. J., and J. K. Blasie. 1989. Effect of Mg^{+2} concentration on the Ca^{+2} uptake kinetics and structure of the sarcoplasmic reticulum membrane. *Biophys. J.* 55:739–753.
4. Pierce, D., A. Scarpa, D. Trentham, M. Topp, and J. K. Blasie. 1983. Comparison of the kinetics of calcium transport in vesicular dispersions and oriented multilayers of isolated sarcoplasmic reticulum membranes. *Biophys. J.* 44:365–373.
5. Luzzati, V., and A. Tardieu. 1974. Lipid phases: structure and structural transitions. *Ann. Rev. Phys. Chem.* 25:79–94.
6. Levine, Y. K., and H. F. Wilkins. 1971. Structure of oriented lipid bilayers. *Nature New Biol.* 230:69–72.
7. McFarland, B., and G. Inesi. 1971. Solubilization of sarcoplasmic reticulum with triton X-100. *Arch. Biochem. Biophys.* 145:456–464.

8. Meissner, G., G. Conner, and S. Fleischer. 1973. Isolation of sarcoplasmic reticulum by zonal centrifugation and purification of Ca^{+2} pump and Ca^{+2} binding proteins. *Biochim. Biophys. Acta.* 298:246–269.

9. Herbette, L., A. Marquardt, A. Scarpa, and J. K. Blasie. 1977. A direct analysis of lamellar x-ray diffraction from hydrated oriented multilayers of fully functional sarcoplasmic reticulum. *Biophys. J.* 20:245–272.

10. Rouser, G., and S. Fleischer. 1967. Isolation, characterization and determination of polar lipids of mitochondria. *Methods Enzymol.* 10:385–406.

11. Rouser, G., S. Fleischer, and A. Yamamoto. 1970. Two dimensional thin layer chromatographic separation of polar lipids and determination of phospholipids by phosphorus analysis of spots. *Lipids.* 5:494–496.

12. Hidalgo, C., D. Thomas, and N. Ikemoto. 1978. Effect of the lipid environment on protein motion and enzymatic activity of the sarcoplasmic reticulum calcium atpase. *J. Biol. Chem.* 253:6879–6887.

13. Franks, A. 1955. An optically focusing x-ray diffraction camera. *Proc. Phys. Soc. London Sect. B* 68:1054–1064.

14. Cowley, J. M. 1981. Diffraction physics. 2nd ed. North Holland Publishing Co., Amsterdam. 430 pp.

15. Henderson, R. 1975. The structure of the purple membrane from *Halobacterium halobium:* analysis of the x-ray diffraction pattern. *J. Mol. Biol.* 93:123–138.

16. Brady, G. W., D. Fein, M. Harder, R. Spehr, and G. Meissner. 1981. A liquid diffraction analysis of sarcoplasmic reticulum. I. Compositional variation. *Biophys. J.* 34:13–34.

17. Schwartz, S., J. Cain, E. Dratz, and J. K. Blasie. 1975. An analysis of lamellar x-ray diffraction from disordered membrane multilayers with application to data from retinal rod outer segment. *Biophys. J.* 15:1201–1233.

18. Ladd, M. F., and R. A. Palmer. 1985. Structure Determination by X-ray Crystallography. 2nd ed. Plenum Press, New York. 437 pp.

19. Gruner, S., K. Rothschild, and N. Clark. 1982. X-ray diffraction and electron microscope study of phases separation in rod outer segment photoreceptor membrane multilayers. *Biophys. J.* 39:241–251.

20. Joy, R. T., and J. B. Finean. 1963. A comparison of the effects of freezing and of treatment with hypertonic solutions on the structure of nerve myelin. *J. Ultrastruc. Res.* 8:264–282.

21. Kirschner, D. A., and D. L. Caspar. 1975. Myelin structure transformed by dimethylsulfoxide. *Proc. Natl. Acad. Sci. USA.* 72:3513–3517.

22. Bick, R. G., B. Van Winkle, C. Tate, M. Entman, J. K. Blasie, and L. Herbette. 1987. Phospholipid fatty acyl chain asymmetry in the membrane bilayer of isolated skeletal muscle sarcoplasmic reticulum. *Biochemistry.* 26:4831–4836.

23. Davis, D., G. Inesi, and T. Gulik-Krzywicki. 1976. Lipid molecular motion and enzyme activity in sarcoplasmic reticulum membrane. *Biochemistry.* 15:1271–1276.

24. Wieslander, A., J. Ulmius, G. Lindblom, and K. Fontel. 1978. Water binding and phase structures for different *Acholeplasma Laidlawii* membrane lipids studied by deuteron nuclear magnetic resonance and x-ray diffraction. *Biochim. Biophys. Acta.* 512:241–253.

25. Mendelsohn, R., G. Anderle, M. Jaworsky, H. Mantsch, and R. Dluhy. 1984. Fourier transform infrared spectroscopic studies of lipid-protein interaction in native and reconstituted sarcoplasmic reticulum. *Biochim. Biophys. Acta.* 775:215–224.

26. Lentz, B. R., K. W. Clubb, D. R. Alford, M. Hochli, and G. Meissner. 1985. Phase behavior of membranes reconstituted from dipentadecanoyl-phosphatidylcholine and the Mg^{+2} dependent, Ca^{+2} stimulated adenosinetriphosphatase of sarcoplasmic reticulum: evidence for a lipid domain surrounding protein. *Biochemistry.* 24:433–442.

27. Moore, B. M., B. R. Lentz, M. Hochli, and G. Meissner. 1981. Effect of lipid membrane structure on the adenosine 5′-triphosphate hydrolyzing activity of the calcium stimulated adenosinetriphosphatase of sarcoplasmic reticulum. *Biochemistry.* 20: 6810–6817.

28. Bigelow, D., and D. Thomas. 1987. Rotational dynamics of lipid and the Ca^{+2}ATPase in sarcoplasmic reticulum. *J. Biol. Chem.* 262:13449–13456.

29. Squier, T., D. Bigelow, and D. Thomas. 1988. Lipid fluidity directly modulates the overall protein rotational mobility of the Ca^{+2}ATPase in sarcoplasmic reticulum. *J. Biol. Chem.* 263:9178–9186.

30. Caffrey, M., and G. W. Feigenson. 1981. Fluorescence quenching in model membranes, 3: Relationship between calcium adenosinetriphosphatase enzyme activity and the affinity of the protein for phosphatadylcholines with different acyl chain characteristics. *Biochemistry.* 20:1949–1961.

31. Blasie, J. K., L. Herbette, D. Pascolini, D. Pierce, V. Skita, and A. Scarpa. 1985. Time-resolved x-ray diffraction studies of the sarcoplasmic reticulum during active transport. *Biophys. J.* 48:9–18.

32. Blasie, J. K., D. Pascolini, F. Asturias, L. Herbette, D. Pierce, and A. Scarpa. 1989. Large-scale structural changes in the sarcoplasmic reticulum atpase are essential for Ca^{+2} active transport. *Brookhaven Symposium in Biology No. 35.* Synchrotron Radiation in Structural Biology. Plenum Press, New York. pp 77–82.

33. Pascolini, D., L. Herbette, V. Skita, F. Asturias, A. Scarpa, and J. K. Blasie. 1988. Changes in the sarcoplasmic reticulum membrane profile induced by enzyme phosphorylation to $E_1 \sim P$ at 16 Å resolution via time-resolved x-ray diffraction. *Biophys. J.* 54:679–688.

34. Linden, C. D., K. Wright, H. McConnell, and C. Fox. 1973. Lateral phase separations in membrane lipids and the mechanism of sugar transport in *Escherichia coli. Proc. Natl. Acad. Sci. USA.* 70:2271–2275.

35. Wu, S. H., and H. McConnell. 1973. Lateral phase separations and perpendicular transport in membranes. *Biochem. Biophys. Res. Comm.* 55:484–491.